ELSEVIER

Polymer 40 (1999) 5079–5094

polymer

Post-deposition ageing reactions differ markedly between plasma polymers deposited from siloxane and silazane monomers

Thomas R. Gengenbach*, Hans J. Griesser

CSIRO Molecular Science, Bag 10, Clayton South, Victoria 3169, Australia

Received 7 August 1998; received in revised form 2 October 1998; accepted 9 October 1998

Abstract

Plasma polymer coatings deposited from hexamethyldisiloxane (HMDSO) and hexamethyldisilazane (HMDSA) were monitored by XPS, FTIR and contact angle (CA) measurements as they aged in air after fabrication. Of particular interest was the influence of the monomer structure on the long term properties of the plasma deposited materials: in conventionally synthesized organosilicon materials, the siloxane unit provides very good long-term stability whereas the silazane structure is prone to hydrolytic attack. During plasma deposition of both coatings, abstraction of methyl groups was the major activation mechanism and the monomer structure was retained to a substantial extent. In the case of plasma polymerised (pp) HMDSA, however, other reactions such as Si–N bond cleavage resulted in considerably more structural diversity. During storage in air, the ppHMDSO film underwent minor chemical changes such as incorporation of additional siloxane cross-links and a small extent of loss of methyl groups. The chemical structure of both the freshly deposited material and the aged coating were unusually homogeneous, compared with the broad range of chemical structures typically found in most other plasma polymers. The structure of the ppHMDSA coating, in contrast, changed dramatically on ageing: almost all silazane moieties were lost after one year and substantial amounts of oxygen incorporated, mainly in the form of siloxane links. In spite of the initial chemical differences, the two materials became more similar over time, with the final structures of the aged materials based on a cross-linked siloxane backbone. The wettability data reflected the structural differences between the two materials. However, correlations between structures and surface properties were not predictable. The overall wettability of these surfaces was determined by a complex balance of several factors such as chemical structure, topography and mobility.

Keywords: Plasma polymers; Hexamethyldisiloxane; Hexamethyldisilazane

1. Introduction

Polymeric thin films deposited from organosilicon radio-frequency plasmas hold the prospect of combining advantageous properties, such as chemical inertness, of organosilicon compounds such as poly(dimethylsiloxane) with the attractive features offered by plasma-polymerised thin films, such as excellent uniformity and adhesion to substrates. Scientific and commercial interest in the study and development of these materials has therefore been strong [1–16]. A comprehensive review by Wróbel and Wertheimer lists many actual and potential applications for organosilicon plasma polymers, such as protective coatings on optical devices, integrated optics, semiconductor devices, sensor and transducer coatings, electrochemical applications, biomedical applications, permselective membranes and vapour barriers, adhesion promotion and others [17].

Ultimately, however, the usefulness of plasma-deposited coatings depends on whether their properties are maintained throughout the lifetime of the device. While most other aspects of these coatings have been investigated thoroughly, the question of the long-term stability of organosilicon plasma polymers has only been addressed in one early study [3]. Using attenuated total reflection infrared spectroscopy (ATR IR) structural changes were monitored in coatings deposited from three monomers: hexamethyldisilane (HMDS), hexamethyldisiloxane (HMDSO) and hexamethyldisilazane (HMDSA). IR data revealed the formation of –OH, > C=O, Si–O–Si and Si–O–C groups and the decay of SiH groups to be general trends in the ageing of these three materials. They were ascribed to reactions of atmospheric oxygen and water with alkyl and silyl radicals as well as with other reactive bonds present in the plasma polymers after deposition. The effects of these chemical changes on surface properties were followed by contact

* Corresponding author. Tel.: + 61-3-9545-2593; fax: + 61-3-9545-2446.

E-mail address: thomas.gengenbach@molsci.csiro.au (T.R. Gengenbach)

0032-3861/99/$ - see front matter
PII: S0032-3861(98)00727-7

angle measurements, and were found to consist of an increase in the polar component and a decrease in the dispersive component of the surface free energy.

Modern spectroscopic methods such as X-ray Photoelectron Spectroscopy (XPS) provide additional tools for study of the long-term ageing of plasma deposited coatings. In addition, XPS provides quantitative information on the amounts of chemical groups present, whereas ATR-IR spectra are subject to polarization effects for which it can be difficult to compensate in materials as complex as plasma polymers. We have previously investigated the spontaneous extended, ambient post-plasma ageing of plasma deposited coatings based on hydrocarbon [18], alkylamine [19–21], acrylate [22] and fluorocarbon monomers [23], as these materials were stored in ambient air for up to 4 years after fabrication. Using XPS in combination with FTIR and contact angle measurements we were able to elucidate the chemical reaction products that arise at various times of storage in the oxidative ageing process, which consists of a complex set of reaction cycles. However, the ageing of these materials usually did not only involve oxidative chemical changes; the physical process of surface restructuring also took place over time and led to observable changes in contact angles. This surface mobility was corroborated by angle-resolved XPS analyses which proved to be particularly valuable in providing direct information about the depth distribution of chemical species; we were thus able to show that the wettability of these plasma polymers is governed not only by oxidative chemical changes occurring in the surface layers but also by rearrangements of polymeric segments at the plasma polymer surface as the materials age. The time-dependent surface properties were determined by the overall balance of the two concurrent, competing processes.

While Wróbel's study [3] demonstrated the occurrence of oxidative chemical changes, it is not clear from his data to what extent surface restructuring may have played a role in the evolution of the surface chemical composition and properties. Also, Si–N bonds can be unstable in oxidative environments but it is not clear from that study what the fate is of silazane bonds during ageing. We therefore decided to perform a comparative multitechnique study of coatings deposited from HMDSO and HMDSA plasmas to address a number of questions. Firstly, we probed for reaction mechanisms and the kinetics of oxidation quantitatively by XPS, supported by qualitative IR data to compensate for the inability of XPS to distinguish between some chemical groups of interest. Secondly, we aimed to study the relative contributions of oxidative reactions and surface restructuring in determining the chemical composition of the top few nanometres of the material and thus its surface properties, by angle-resolved XPS data and contact angle measurements.

HMDSO and HMDSA were plasma polymerised under identical plasma conditions. A low plasma power ensured maximum retention of the monomer structure in the resulting polymeric films; for these monomers it is well known that high plasma power leads to extensive monomer fragmentation in the glow discharge and, consequently, to films of a more or less inorganic nature [5,14]. The juxtaposition of HMDSO and HMDSA promised to give valuable information regarding the influence of the monomer structure on the various ageing processes. Despite the very similar chemical structure of HMDSO and HMDSA, the conventionally synthesized polymers show dramatically different long-term stability: whereas poly(organosiloxanes) are very resistant to heat, radiation and oxidation, their silazane analogues are unstable due to the reactivity of the Si–N bond in protic solvents such as water. As a consequence, the former have found a wide variety of applications while the latter are mainly used as precursors for silicon nitride (Si_3N_4) and silicon carbonitride [24]. We aimed to study whether the long-term stability of HMDSO and HMDSA plasma polymers would also differ so markedly.

2. Experimental sample preparation

2.1. Substrate

The substrate for plasma deposition was a polyimide web (Kapton 100HN, 25 μm thick, 12.7 mm wide) which had been coated with approximately 0.1 mm of aluminium by electron beam evaporation. The highly reflective aluminium surface not only provides a good substrate for FTIR analysis (specular reflectance mode) but also facilitates estimating the thickness of the plasma polymer films by observing the interference fringes.

2.2. Monomer

Plasma polymer films were deposited using hexamethyldisiloxane $(CH_3)_3Si–O–Si(CH_3)_3$ (HMDSO, 99.5 + % purity, Aldrich) and hexamethyldisilazane $(CH_3)_3Si–NH–Si(CH_3)_3$ (HMDSA, 99.9% purity, Aldrich) as the feed monomers. A fresh batch of the monomer liquid was placed in a round bottom flask and connected to the reactor chamber by a stainless steel line and a manual flow control valve. Volatile impurities were removed by pumping on the liquid for a few minutes prior to ignition of the plasma.

2.3. Plasma deposition

Plasma depositions were carried out in a reactor of conventional design; it employed two capacitively-coupled parallel disc-shaped electrodes in a horizontal configuration within a cylindrical glass vessel (7.4 l volume). Samples were placed on the base electrode (155 mm diameter, earthed) for the treatment. The upper electrode (active) was separated from the lower electrode by ca. 150 mm. The oscillator used in this study was a commercial plasma generator (ENI model ACG-3) operating at 13.56 MHz and equipped with a matching network. Identical conditions

were chosen for the deposition of the two plasma polymers: reactor base pressure, 0.03 mbar; initial monomer pressure, 0.15 mbar; plasma load power, 50 W; plasma frequency, 13.56 MHz; deposition time, 450 s. As is typical for plasma depositions with many monomers in our system, there occurred a gradual rise in pressure after ignition of the plasma. The maximum monomer pressure, reached about 30 s after ignition of the plasma, was 0.17 mbar for HMDSO and 0.24 mbar for HMDSA.

The uniformity of the deposition was assessed by XPS analysis of specimens from different locations of the freshly coated substrates and by visual examination of the interference fringes. The colour of the latter also allowed an estimation of the thickness of the coatings (several hundred nm). The web was cut into short sections, providing a large number of identical specimens. These were stored in cleaned glass Petri dishes at room temperature (20 ± 1°C); during storage the relative humidity varied between 30% and 70%, and samples were not exposed to sources of UV radiation. They were analysed periodically with the analysis of the first specimen taking place within 10–15 minutes (XPS) and 30–60 minutes (FTIR, CA) of venting the plasma reactor with N_2 and the subsequent exposure to air.

3. Analyses

The multi-technique approach used in this study is essentially identical to that used in our previous analyses of oxidative changes and surface restructuring of other plasma polymers [18,25].

3.1. X-ray photoelectron spectroscopy.

XPS analysis was performed in a Vacuum Generators Escalab V unit with a non-monochromatic Mg K_α source at a power of 200 W (10 kV × 20 mA) and a hemispherical analyser operating in the fixed analyser transmission mode. The total pressure in the main vacuum chamber during analysis was typically 5×10^{-9} mbar. Calibration procedures are detailed in Ref. [18].

Elements present were identified from survey spectra. For further analysis, high resolution spectra were recorded from individual peaks at 30 eV pass energy. The latter data were quantified as described previously [18]. The random error associated with quantification was determined following the method suggested by Harrison and Hazell [26]. It was generally found to be between 2% and 4%. Higher values were estimated for weak photoelectron signals (low signal/noise ratio), between 8% and 10% for the O/Si ratio measured on the freshly deposited ppHMDSA and in excess of 30% for the N/Si ratio measured on the aged ppHMDSA coating. The standard deviations are indicated in corresponding figures as error bars for selected data points. The contribution of systematic errors is difficult to estimate, but was assumed to be small since data acquired with another XPS unit agreed to within a few percent. This second instrument, which became available later in the study, is an AXIS HSi spectrometer (Kratos Analytical Inc., Manchester, UK) and was used with the monochromated Al K_α source at a power of 300 W (15 kV × 20 mA) and the hemispherical analyser operating in the fixed analyser transmission mode.

The results presented in this report were obtained at two photoelectron emission angles (0° and 75° with respect to the surface normal). Only recently has the electron attenuation length been determined experimentally for a similar plasma polymerised material [27]; assuming that the organosilicon plasma polymers had similar physical properties (density etc.), approximate values for the attenuation length range from 2.1 nm (Si 2p photoelectrons) to 1.5 nm (O 1s). Thus, the depth from which 95% of the detected XPS signal originates is approximately 4.5–6 nm at 0° emission and 1.5–2 nm at 75°. Some uncertainty arises because of non-ideal sample topography: since the coatings are not perfectly flat, the macroscopically measured photoelectron emission angle corresponds to a range of angles on a microscopic scale. All data presented in this report were acquired at an emission angle of 0° with respect to the surface normal unless stated otherwise.

The effects of sample decomposition under X-radiation, particularly with unmonochromatized radiation, have been considered. Specimens were exposed to X-radiation less than one minute before the start of the actual data acquisition. Total exposure time never exceeded 30 min; changes to the elemental composition due to sample degradation were thus kept below 5%. To avoid the accumulation of radiation damage due to repeated XPS analysis of the same specimen over longer time periods, new specimens were cut from the same web for each analysis. Hence the importance of preparing a large number of identical specimens as outlined above.

The uncertainty involved in measuring photoelectron peak binding energies (BEs) was estimated according to a protocol presented earlier [20]. The standard deviation with respect to BE measurements was found to be ± 0.15 eV. It is indicated in corresponding figures as error bars for selected data points.

In order to determine absolute BE values of photoelectron peaks one has to correct the measured peak positions for the inevitable charging of insulating samples during analysis. Commonly, the C 1s BE of aliphatic hydrocarbons (285.0 eV) is used in the surface analysis of polymers as an internal reference value. In the case of organosilicon polymers, however, the C 1s BE for CH_3–Si is lowered by the adjacent silicon to 284.38 eV–284.39 eV [28]. Although the presence of more extended hydrocarbon segments was indicated in the case of the ppHMDSA material (evidence presented in Section 4), for the sake of consistency a value of 284.4 eV was assumed for the main C 1s signal throughout this study.

Identification of chemical species by XPS relies on prior knowledge of BE reference values. Relevant BEs reported

Table 1
Compilation of corrected reference BE values collated from the literature (see text for details)

Photoelectron line	Structure (Chemical species)	Mean BE (eV)	Standard deviation (eV)
O 1s	$-(Si(CH_3)_2-O)_n-$ (Siloxane)	532.11	0.12
O 1s	SiO_2 (Silica)	532.93	0.34
N 1s	=N–Si≡	397.80	N/A[a]
Si 2p	=N–Si≡	101.20	N/A[a]
Si 2p	≡Si–Si≡, ≡Si–C≡	100.61	0.38
Si 2p	$-(Si(CH_3)_2-O)_n-$ (Siloxane)	102.15	0.36
Si 2p	SiO_2 (Silica), –O–Si(O) –O–	103.49	0.13

[a] Only one entry.

in earlier studies [1,2,7,9,11–14,28–32] vary somewhat; most commonly, BE values were referenced to the C 1s BE of C–Si but the actual value used for this component by different workers ranged from 284.3 eV to 285.2 eV. Better agreement between the various literature data is obtained when one re-adjusts published BE values for other elements based on a common value of 284.4 eV for C–Si [28]. Table 1 lists mean BE values and standard deviations calculated thus from published data. These values were used as BE reference values for interpretation of our experimental data.

Assessing subtle changes to the shape of photoelectron peaks by monitoring the peak width can provide additional qualitative information in cases where curve fitting is not possible [23]. The half width at half maximum (HWHM) was determined on either side of relevant peaks (FWHM = low BE HWHM + high BE HWHM) for the first 3 measurements after plasma deposition (fresh samples) and the last 3 measurements (aged samples) both at 75° emission and at 0° emission. The mean values were calculated in the case of fresh and aged coatings, respectively; standard deviations ranged from 0.01 eV to 0.04 eV.

3.2. Curvefitting XPS spectra

Individual spectral components arising from different chemical species or bonding configurations were quantified using damped non-linear least-squares regression (curvefitting). The customized software used is based on a curvefitting algorithm by Hughes and Sexton [33] and uses a Gaussian/Lorentzian product function for individual spectral components. The Gaussian/Lorentzian mixing ratio and the peak width were constrained to have the same (but adjustable) value for all components. The specific curvefit protocols including additional constraints are described in Section 4 where appropriate. Since for this report results of curvefitting are presented in a qualitative rather than quantitative fashion, an error analysis, as in previous publications, [19] was deemed unnecessary.

3.3. Infrared spectroscopy

Infrared spectra of the plasma polymer films were measured on a BOMEM MB-100 FTIR spectrometer fitted with a SpectraTech FT80 Specular Reflectance attachment using a fixed grazing angle of 80°. Spectra were scanned 128 times with a resolution of 8 cm^{-1} to increase the Signal/Noise ratio. Since the instrumental contribution to peak broadening in FTIR spectra of plasma polymers is less significant than intrinsic effects, a higher instrumental resolution only reduced the S/N ratio without any beneficial effect concerning the overall resolution. In order to enhance small spectral changes due to chemical changes in the analysed material over time, most FTIR spectra will be presented as difference spectra. The spectrum of the freshly deposited plasma polymer film, which is used as a reference, is subtracted from spectra recorded at various intervals during storage. Reference spectra were recorded with the monomer liquids as neat films between NaCl plates in transmission at a resolution of 2 cm^{-1}. Absorption bands were assigned based on reference infrared group frequencies [34–36] and relevant earlier studies [1,2,4,7–9,11,13,14,17].

3.4. Contact angle measurements

Contact angles were measured with triply distilled deionized water at various times during storage using a modified Kernco Model G-II goniometer. The goniometer was equipped with a reversible, micrometer driven plunger in the syringe to enable determination of the advancing (q_A) and receding (q_R) contact angles. Readings were taken from four drops and the mean and standard deviation calculated from these values. Clean reference surfaces of fluorinated ethylene propylene copolymer (FEP) were used to ascertain reproducibility of measurements and purity of the water. Separate washing experiments showed that the plasma polymer coatings were coherent and that soluble species, which could have affected the measurements, were not present in detectable quantities on the surface.

3.5. Atomic force microscopy

Atomic force microscopy (AFM) experiments were performed with a Nanoscope III unit (Digital Instruments, Santa Barbara, CA). Microfabricated V-shaped silicon nitride cantilevers with integral square pyramidal tips were employed. AFM images were acquired in the contact

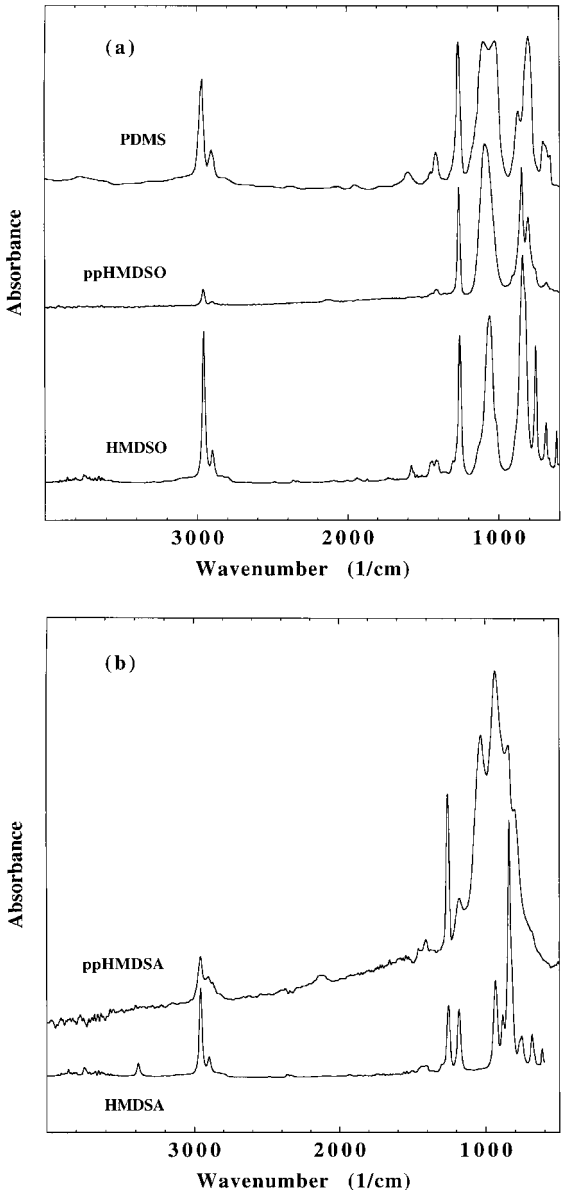

Fig. 1. IR spectra of freshly deposited plasma polymer coatings. (a) ppHMDSO, and reference spectra of HMDSO monomer and PDMS, the latter taken from Ref. [38]; (b) ppHMDSA and reference spectrum of HMDSA monomer.

mode. The Nanoscope III software as well as specialised image analysis software developed by the authors was used to characterise the topography of the coatings and to calculate the root-mean-square (RMS) roughness for individual images.

4. Results and discussion

4.1. Structure of freshly deposited films: ppHMDSO

Quantitative XPS analysis of the surface composition of the freshly polymerised coatings enabled comparison of their composition with both the monomer and conventionally synthesized materials (e.g., polydimethylsiloxane, PDMS). Since the atomic concentration of silicon did not change within experimental uncertainty during ageing (30.5% ± 0.4%), compositional data will be presented relative to Si.

The carbon/silicon (C/Si) atomic ratio of 1.65 was about half that of the monomer (C/Si = 3) and less than the value for PDMS (C/Si = 2); the oxygen/silicon (O/Si) ratio of 0.52 was about the same as for the monomer and half the value for PDMS. Clearly, the polymerisation processes taking place in the glow discharge were very different from the conventional polymerisation of linear polysiloxanes, which is achieved either by chain growth (ring-opening polymerisation of cyclodialkylsiloxanes) or by step growth (e.g., homocondensation of silanol-terminated siloxanes) [37]. Our data suggest abstraction of methyl groups to be the major fragmentation/activation reaction in the glow discharge (substantial loss of carbon), whereas Si–O bonds did not seem to undergo scission to an appreciable extent. Si–O–Si structures appeared to be incorporated intact into the growing film.

The experimentally determined O 1s BE of 531.9 eV is assigned to oxygen in siloxane, Si–O–Si, by comparison with the value of 532.11 eV in Table 1. The measured value for the Si 2p BE (101.7 eV), however, was somewhat lower than expected for siloxane, being between the reference values for silanes Si–Si (100.61 eV (0.38 eV)) and siloxanes (102.15 eV (0.36 eV)) although much closer to the siloxane value. We assume that this signal is a compound line with unresolved contributions from chemically different species. The finding indicates the presence of a range of structures such as $-O-Si(CH_3)_2-O-$ (PDMS), $-O-Si(CH_3)_3$ (as in the monomer HMDSO) or $\equiv Si-Si(CH_3)_2-O-$. The latter could be formed as a product of termination reactions involving two silyl radicals.

The IR spectrum of ppHMDSO (Fig. 1a) was found to be very similar to those of HMDSO and PDMS [38]. The following vibrational bands appeared in the spectra of all three materials: the asymmetric and the symmetric C–H stretch of methyl groups at 2960 cm^{-1} and 2900 cm^{-1}, the $-CH_3$ asymmetric and symmetric deformation of methyl groups in $Si(CH_3)_x$ at 1410 cm^{-1} and at 1262 cm^{-1}, a broad absorption band between 1120 cm^{-1} and 1050 cm^{-1} due to the Si–O–Si stretching vibration and a group of absorptions between 850 cm^{-1} and 650 cm^{-1} originating from various vibrational modes of the $Si(CH_3)_x$ structure, most prominently the methyl rocking mode at 850 cm^{-1} and 805 cm^{-1}.

Interestingly, for ppHMDSO no appreciable absorption assignable to CH_2 groups was observed. This indicates that cleavage of C–H bonds was of little importance in the plasma polymerization of HMDSO even though this is a dominant pathway for monomer activation in plasmas for most other monomers. This accords with the abstraction of C observed by XPS; apparently, cleavage of Si–C bonds is

the dominant plasma activation route for this monomer. However, a weak band between 2150 and 2110 cm^{-1}, assignable to Si–H stretch, is observable in Fig. 1a. The H necessary to form such bonds may not necessarily originate from C–H scissions of monomer molecules; an alternative source may be cleavage of abstracted methyl radicals by secondary plasma reactions. We should note that this band may also be due to an overtone of the very intense Si–O–Si stretch.

Comparing the spectra of ppHMDSO and PDMS we note that the relative intensities of the methyl rocking absorptions at 850 cm^{-1} and 805 cm^{-1} were markedly different. For PDMS the absorption at the lower frequency is much more intense than the higher frequency band; the spectra of the plasma polymerised material, however, showed the band at 850 cm^{-1} to be nearly twice as intense as the absorption at 805 cm^{-1}, akin to the spectrum of HMDSO which has an intense absorption centred at 840 cm^{-1} with a shoulder on the low frequency side. The $Si(CH_3)_3$ structure is characterised by an absorption around 850 cm^{-1}, accompanied by a second band between 760 and 750 cm^{-1}, whose intensity depends on the chain length. The $Si(CH_3)_2$ structure, on the other hand, displays the main methyl rock around 800 cm^{-1} with a second, minor band near 855 cm^{-1} [34]. We conclude that there is a substantial extent of retention of the $Si(CH_3)_3$ structure in ppHMDSO. The plasma polymer therefore does not consist of a linear siloxane backbone but comprises Si–O–Si structures, Si–Si links, and a substantial concentration of $Si(CH_3)_3$ moieties. The O/Si ratio of 0.52 indicates that the material does not consist simply of a siloxane network with pendent methyl groups.

4.2. Structure of freshly deposited films: ppHMDSA

Relative to Si the following composition was determined for the silazane-based material: C/Si = 2.24 and N/Si = 0.36. Both values are approximately 3/4 of those of the monomer. The C/Si ratio again indicated abstraction of methyl groups in the plasma; the value of 2.24 is consistent with the various oligomers which have been proposed to be formed in silazane plasmas [17]. The N/Si ratio is evidence for some Si–N bond scission. Cleavage of Si–NH bonds leads to a wider variety of possible reactions of molecular fragments and, consequently, to a wider variety of chemical structures in the forming plasma polymer. We also note that the pressure rise in the plasma reactor during the first half minute after plasma ignition was considerably higher for HMDSA than for HMDSO (60% vs. 13%) confirming a higher extent of monomer fragmentation in the glow discharge.

The experimental BE values of freshly deposited ppHMDSA were 398.0 eV for N 1s and 101.3 eV for Si 2p. Only two previous publications [1,2] reported XPS BE values for silazane plasma deposited films (Table 1). One may predict a theoretical value for Si–NH–Si by comparison with the oxygen 1s data: the O 1s BE is lowered from 533.1 eV in poly(methylene glycol) $-(-CH_2-\underline{O}-)_n-$ to 532.0 eV in $-(-Si(CH_3)_2-\underline{O})_n-$. If we assume the same reduction of the N 1s BE by adjacent Si atoms and use a value of 399.1 eV for polyethyleneimine $-(-CH_2-CH_2-\underline{NH}-)_n-$, we obtain 398.0 eV for Si–NH–Si, in good agreement with the literature data [1,2]. Using the same method to estimate the expected Si 2p binding energy, we compare with the carbon analogue: the mean value and the standard deviation for literature values of Si 2p BE measured in silanes (Si–C, Si–Si) was 100.61 eV ± 0.38 eV. The C 1s BE of aliphatic hydrocarbon (285.0 eV) is raised by about 0.6 eV in $-(-CH_2-CH_2-\underline{NH}-)_n-$ [28]. Assuming the same shift by NH on the Si 2p BE in silazane, we predict a value of 101.2 eV. Thus, both our and Inagaki's BE values recorded with silazane plasma polymers agree well with theoretical BE predictions. These data are therefore consistent with a substantial density of Si–N bonds in the materials.

The infrared spectrum of ppHMDSA (Fig. 1b) showed some features common with ppHMDSO: the C–H stretch of methyl groups at 2960 cm^{-1} (ν_a) and 2900 cm^{-1} (ν_s), the Si–H stretch between 2150 cm^{-1} and 2100 cm^{-1}, the $-CH_3$ deformation in $Si(CH_3)_x$ at 1410 cm^{-1} (δ_a) and at 1257 cm^{-1} (δ_s) and various vibrational modes of the $Si(CH_3)_x$ structure between 850 cm^{-1} and 650 cm^{-1}, e.g., the methyl rocking modes at 845 cm^{-1} and 805 cm^{-1}. In addition, the following absorptions were observed: the in-phase C–H stretching vibration of methylene units between 2930 cm^{-1} and 2920 cm^{-1} and the corresponding out-of-phase mode at 2870 cm^{-1}. A related band appeared at about 1035 cm^{-1}, assigned to the CH_2 wag in $Si-CH_2-Si$ and $Si-CH_2-CH_2-Si$ links. Absorptions associated with nitrogen were detected at 1180 cm^{-1} (NH bend) and at 935 cm^{-1} (Si–NH–Si stretch). We note, however, that the intensity of absorptions due to the N–H bond (stretching mode at about 3400 cm^{-1} and bending mode at 1180 cm^{-1}) was markedly reduced compared to the spectrum of the monomer. In the latter case, the NH bend and the adjacent absorption due to the symmetric deformation vibration of the methyl group are of similar intensity [38]. In the case of the plasma polymerised material the band at 1180 cm^{-1} was rather weak and hardly any absorption was detected above 3000 cm^{-1}. We conclude that apart from Si–N bond cleavage, hydrogen abstraction from NH was also a major process during plasma deposition. This could then lead to branched structures of the form Si(R1)–N(SiR2)–Si(R3) or Si(R1)–N(R2)–Si(R3). Hydrogen atoms were also abstracted from methyl groups as evidenced by the appearance of vibrational bands due to $-CH_2-$ units. Thus, there is considerably more structural diversity in ppHMDSA compared with ppHMDSO, which is in agreement with results of a pyrolysis/gas chromatography/mass spectrometry study of siloxane and silazane plasmas [17].

The question arises why hydrogen abstraction from methyl groups occurred in HMDSA but not in HMDSO. We propose that Si–N bonds cleave during plasma

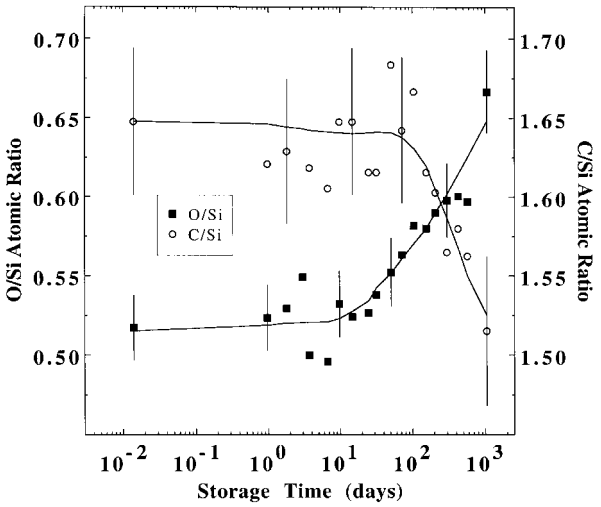

Fig. 2. XPS O/Si (■) and C/Si (○) ratios as a function of storage time for ppHMDSO.

deposition and generate $N^{\cdot}$ radicals which form ammonia by abstracting hydrogen atoms from methyl groups. In the case of the HMDSO plasma our data did not indicate Si–O scission to be an important activation process and therefore H abstraction by $O^{\cdot}$ radicals did not occur to a similar extent.

4.3. Structural changes during ageing: ppHMDSO

The compositional changes observed during storage of the ppHMDSO film by XPS are presented in Fig. 2. A logarithmic time scale was chosen in order to show short-term as well as long-term changes. The following discussion of oxidative ageing is based on the data acquired at normal emission; more surface sensitive data recorded at 75° emission were in agreement and will be presented below to assess surface restructuring. Both the C/Si and O/Si ratios changed by about the same amount ($\Delta C/Si = -0.12$, $\Delta O/Si = +0.13$) suggesting simultaneous loss of carbon (further

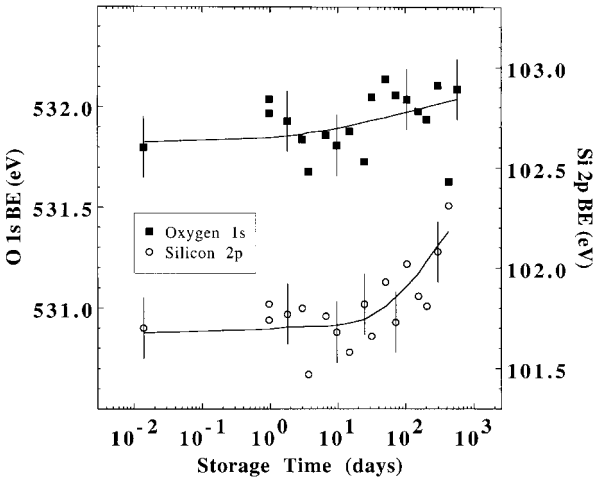

Fig. 3. XPS BE values of O 1s (■) and Si 2p (○) as a function of storage time for ppHMDSO.

abstraction of methyl groups) and incorporation of additional oxygen. However, the kinetics of the observed changes differed: the O/Si ratio started to increase after the first few days, whereas the C/Si ratio only started to decrease appreciably after about three months. This suggests that at least two different processes affected the chemical structure of the ppHMDSO over time.

An interesting feature is that the oxygen content did not increase measurably during the first few days; this is in marked contrast to other plasma polymer whose ageing we have studied [18–23], where invariably rapid incorporation of oxygen was measured during the first day. This initial fast rise in the oxygen level can be attributed to reaction between trapped, carbon-centered radicals in the plasma polymer with O_2 diffusing into the material. It follows that our ppHMDSO coating did not contain a comparable concentration of trapped radicals. Termination reactions such as for example $\equiv Si^{\cdot} + {}^{\cdot}Si\equiv \rightarrow \equiv Si–Si\equiv$ must have been very efficient during the plasma deposition to quench remaining radicals. This unusual observation can be rationalized by considering the unique characteristics of the Si–O–Si structure. Poly(dimethylsiloxane) is one of the most flexible chain molecules known, with the lowest glass transition temperature recorded for any polymer. The Si–O bond length of 1.64 Å is significantly longer than that of a C–C bond (1.53 Å), i.e., steric interferences are diminished. Oxygen atoms are small and unobstructed by side groups. The Si–O–Si bond angle of ≈143° is much more open than the usual tetrahedral bond angle of ≈110° [37]. We expect this extreme chain flexibility to be partially retained in the HMDSO plasma polymer; the resulting mobility appears to have been sufficient to eliminate the majority of trapped radicals in the polymeric structure.

Binding energy values are displayed in Fig. 3; they remained constant within experimental uncertainty (O 1s BE at 532.0 eV) or increased slightly (Si 2p from 101.7 eV to 102.2 eV). The final BE values are consistent with silicon and oxygen in siloxane. The peak shapes and widths of the O 1s and C 1s photoelectron peaks remained unchanged; they were both symmetrical with a width (FWHM) between 1.8 and 1.9 eV. The Si 2p peak measured on the freshly deposited material was slightly asymmetrical (1.21 eV on the low BE side, compared to 1.12 eV on the high BE side). After extended storage the signal assumed a symmetrical shape, but the overall width (FWHM) remained constant at about 2.3 eV. The initial asymmetry can be assigned to the presence of silicon bonded to only one oxygen atom, and oxidation reactions appear to lead to the disappearance of these groups after extended periods of time. This indicates that structures such as $\equiv Si–Si(CH_3)_2–O–$ or $CH_3–Si(CH_3)_2–O–$ formed in the glow discharge were gradually being replaced by siloxane units $–O–Si(CH_3)_2–O–$.

Fig. 4 displays IR spectra recorded at various times during storage. The main changes detected by IR during storage concerned the Si–O–Si stretching vibration and

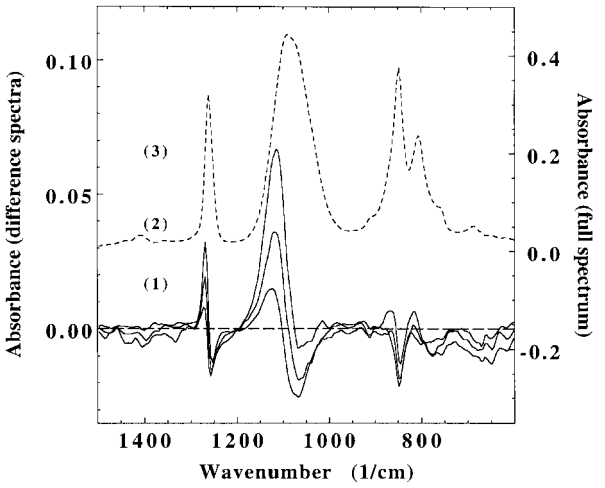

Fig. 4. IR difference spectra of the ppHMDSO film recorded at various times during storage: after 80 days (1), 154 days (2) and 589 days (3). Spectra recorded at intermediate times not shown. The spectrum of the freshly deposited coating is included for comparison (dashed curve).

the absorptions associated with $Si(CH_3)_x$ species: the Si–O–Si stretch displayed an increase in absorption on the high frequency side (around 1115 cm^{-1}) and a decrease in absorption on the low frequency side (around 1065 cm^{-1}), the latter particulary noticeable between 3 and 5 months after deposition. The doublet nature is due to a symmetric (higher frequency) and an asymmetric (lower frequency) Si–O–Si stretch component [39]. The net effect on the Si–O–Si stretching band was an overall increase in absorption and a shift by about 10–20 cm^{-1} to higher frequency. The overall intensity increase of this compound band indicates that more Si–O–Si bonds (cross-links) were formed as a consequence of ageing, however, the different evolution of the symmetric and asymmetric Si–O–Si stretch absorptions is currently not understood.

A similar evolution was observed for the band at around 1260 cm^{-1}: a decrease at 1254 cm^{-1} and an increase at 1269 cm^{-1} resulted in an overall shift of this absorption to higher frequency. This band is actually a doublet, consisting of the main band at 1262 cm^{-1} (characteristic of all $-Si(CH_3)_x$ groups) and an absorption at about 1250 cm^{-1}, which is observed only for trimethylsilyl structures. The observed shift therefore indicates a decrease in the number of $-Si(CH_3)_3$ units over time, consistent with XPS data. This is further confirmed by the observed change of the methyl rocking absorption: the intensity of the main band at 850 cm^{-1} was reduced during storage, as was the absorption intensity between 760 cm^{-1} and 750 cm^{-1} (both indicative of $-Si(CH_3)_3$ groups). These reductions in absorption intensity due to the abstraction of methyl groups all took place mainly between the 3rd and the 5th month of storage; this is consistent with the loss of carbon detected by XPS after about 3 months.

After extended periods of storage the Si–H stretching band disappeared, providing evidence for hydrogen

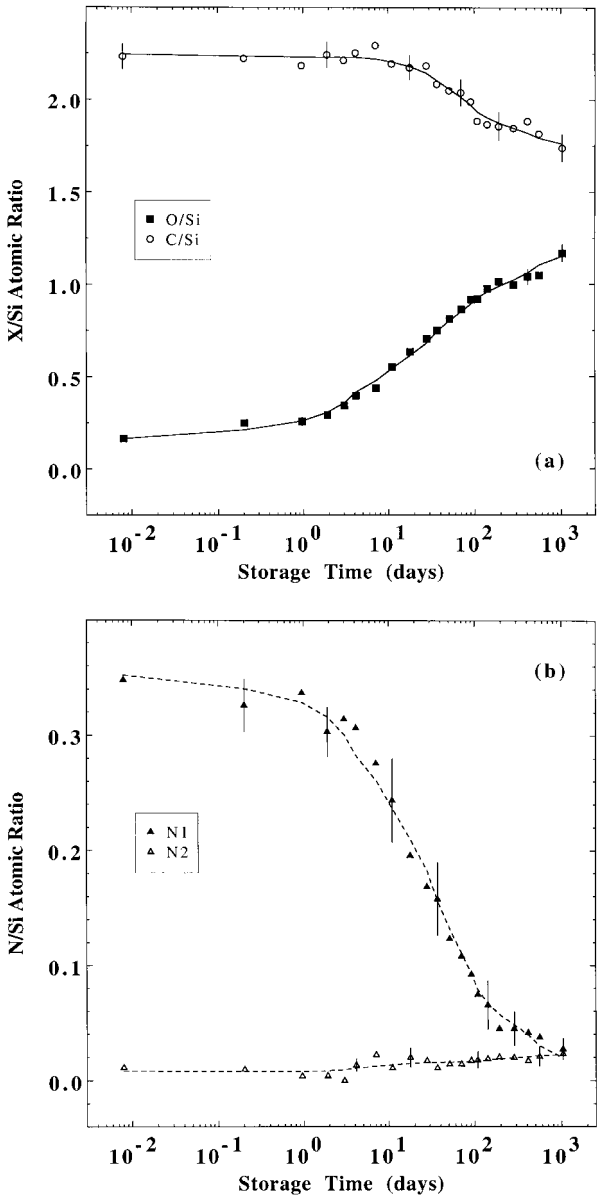

Fig. 5. XPS X/Si ratios as a function of storage time for ppHMDSA. (a) O/Si (■) and C/Si (○), (b) N1/Si (▲) and N2/Si (△). See text for details regarding N 1s curvefitting.

abstraction from Si atoms; this could result in the formation of additional siloxane units according to $2{\equiv}Si{-}H + O_2 \rightarrow 2{\equiv}Si{-}OH \rightarrow {\equiv}Si{-}O{-}Si{\equiv} + H_2O$.

Based on these data we can draw the following conclusions. The freshly deposited coating did not contain a measurable concentration of free radicals, which in other plasma polymers provide the sites for initial oxygen incorporation into the material upon exposure to atmosphere. Instead, Si–Si-based structures proved to be the most reactive species in the ppHMDSO coating. Hydrolysis of Si–Si bonds followed by the formation of silanols and secondary condensation reactions leading to siloxane moieties was proposed by Wróbel as being particularly important in the ageing of silane plasma polymers [3]. Also, studies of the

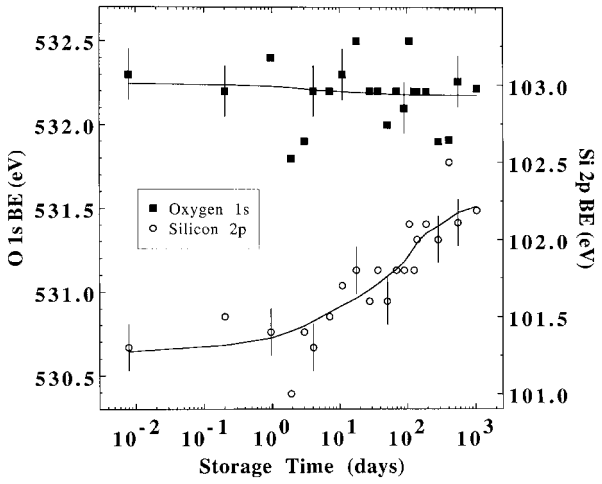

Fig. 6. XPS BE values of O 1s (■) and Si 2p (○) as a function of storage time for ppHMDSA.

radiation sensitivity of poly(silanes) have shown that Si–Si bond homolysis is the main process upon UV-irradiation of these materials. The silyl radicals are then scavenged by oxygen to produce predominantly silanols and siloxanes [37]. Analogously, Si–Si bonds incorporated into our ppHMDSO appear to be the main sites for slow reactions during storage.

After several months a second process started to affect the ppHMDSO structure, characterised by the loss of methyl groups and incorporation of additional Si–O–Si links. These changes did not lead to a markedly different chemical structure of the ppHMDSO coating, even after ageing for almost three years. Rather, the structure evidently became more uniform and similar to its conventional analogue PDMS.

4.4. Structural changes during ageing: ppHMDSA

Some oxygen (O/Si = 0.17) was detected in the freshly deposited film which might have been partially due to oxygen impurities in the discharge and/or to exposure to atmosphere. The O 1s BE of 532.3 eV, which was somewhat higher than expected for Si–O–Si probably indicated the presence of various oxygen-containing structures such as Si–O–Si, Si–O–C and O–C structures. A low concentration of C–O bonds was indicated by a weak C 1s signal detected at somewhat higher binding energy (about 1 to 2 eV) than the main carbon peak.

The chemical changes during storage for ppHMDSA were much more extensive compared to ppHMDSO. The O/Si ratio increased from 0.17 to about 1.15, accompanied by the almost complete loss of nitrogen, with N/Si decreasing from 0.36 to about 0.05, as shown in Fig. 5. A decrease of the C/Si ratio was also observed, from 2.24 to 1.75. The increase in O (ΔO/Si = 0.98) was somewhat higher than the combined loss of N and C (ΔN/Si + ΔC/Si = −0.80). In contrast to the corresponding ppHMDSO data, the O/Si ratio increased significantly during the first day (ΔO/Si = + 0.08 within the first five hours). This evolution is similar to the oxidative ageing of other plasma polymers, where the amount of oxygen incorporated (ΔO/C) during the initial, very rapid phase of oxidation was in the range 0.04 to 0.07 [18–20]. This first stage of oxidation after deposition was assigned to the quenching of radicals in the plasma polymers by O_2 on exposure of the material to air. We therefore propose the same interpretation for the ppHMDSA coating.

More specific information was obtained by monitoring the evolution of peak shapes and BEs of the relevant photoelectron signals: Fig. 6 displays the BE values measured for the O 1s and Si 2p signals (referenced to C 1s at 284.40 eV). Whereas the O 1s BE did not change measurably, the Si 2p BE increased by approximately 1 eV to about 102.2 eV. The latter value is indicative of siloxane units. However, the overall Si 2p peak width increased from about 2.4 eV to approximately 2.7 eV during storage whereas in the case of the ppHMDSO coating this value remained unchanged at 2.3 eV. It follows that in the ppHMDSA material siloxane units were present in a variety of structural environments, in contrast to the ppHMDSO film which had a more uniform structure.

The N 1s signal developed into a doublet. The two components were quantified using the following curvefit protocol: all N 1s spectra were fitted with a two component model with the position of the two peaks being unconstrained. Based on this first round of fitting, the mean peak separation determined was 2.28 eV ± 0.26 eV. All fits were then reoptimised with the separation of the two components fixed at that value. The BEs of the two components did not change during ageing within experimental uncertainty. While the original component at 398.0 eV (Si–N) lost intensity rapidly, a new component appeared at about 400.0 eV, increasing slowly in peak height until both peaks eventually displayed approximately the same, albeit weak, intensity (Fig. 5). The latter BE value is typical for aged alkylamine-based plasma polymers [19,20] and is characteristic of functional groups where the nitrogen is associated with oxygen on the same C atom, such as amide groups but is too low for oxidized N (nitrites, nitrates).

The C 1s peak, which initially had been symmetrical, developed a distinct tail at higher BE, evidence for some incorporation of oxygen into hydrocarbon structures. Since the additional C 1s components remained rather weak and were not clearly resolved, the newly formed carbon-oxygen-functional groups were quantified by C 1s curvefits using established values for the chemical shifts of C 1s BE components relative to aliphatic hydrocarbon at 285.0 eV (+1.5 eV for C–O, +2.9 eV for C=O and +4.3 eV for O–C=O based groups) [28]. Thus, fits were calculated based on five components with fixed separations from the main peak (C–Si at 284.4 eV) of +0.6 eV (CH_x), +2.1 eV (C–O), +3.5 eV (C=O) and +4.9 eV (O–C=O). For the C–O signal a value of 3.5% ± 1.0% of the total C 1s intensity was obtained. This value did not change within

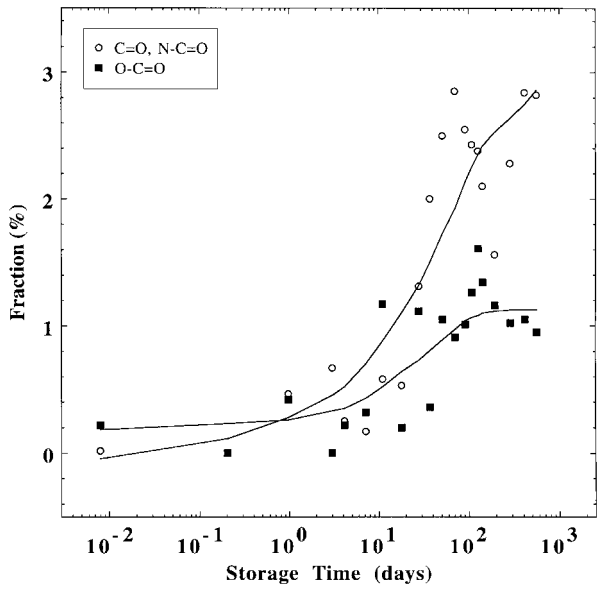

Fig. 7. Evolution of carbonyl (○) and acid/ester (■) groups in the ppHMDSA coating obtained by calculating C 1s curvefits.

experimental uncertainty over time. Fig. 7 displays the evolution of carbonyls/amides and acid/ester groups as a function of storage time. These data, which parallel oxidative changes in other plasma polymers [18,19] but are much less extensive, indicate that oxidation of hydrocarbon moieties occurred.

Hence, ppHMDSA appears to age by loss of silazane groups and their replacement with siloxane cross-links over time, and, in contrast to the ppHMDSO coating, oxidation of methyl groups which produced various carbon–oxygen and carbon–oxygen–nitrogen functional groups.

Fig. 8 presents the changes of the IR absorption recorded at various intervals after deposition of the ppHMDSA coating. The most pronounced changes were the appearance of a new absorption between 1195 cm^{-1} and 1020 cm^{-1} (Si–O–Si stretch) and the simultaneous reduction in intensity of a group of bands centered at 938 cm^{-1}, 870 cm^{-1} (Si–NH–Si stretch) and about 839 cm^{-1} (methyl rock of $-Si(CH_3)_3$). In addition, the following changes are noteworthy. An increase was observed in the NH/OH stretch region (mainly between 3600 cm^{-1} and 3200 cm^{-1}); this is assigned to the OH stretching vibration, given that other absorptions associated with nitrogen-containing structures showed a marked decrease. Since the band was very broad we do not attempt any more specific assignments; possible groups responsible for this absorption are silanols, hydroxyls and carboxylic acid groups. Within the CH stretch region, CH_3-specific absorptions, at 2955 cm^{-1} and at 2900 cm^{-1}, decreased while CH_2-related bands (mainly at 2925 cm^{-1}) increased in absorption. The SiH stretching absorption (2140 cm^{-1}–2100 cm^{-1}) disappeared over time. A new vibrational band appeared between 1720 cm^{-1} and 1700 cm^{-1}; it is assigned to the carbonyl stretch. A shift of the methyl deformation band (sym.) from 1257 cm^{-1} to 1265 cm^{-1} was observed. As in the case of the ppHMDSO material we interpret this shift as indicating a decrease in the number of $-Si(CH_3)_3$ units over time. The corresponding changes of the methyl rocking absorption are also evident in Fig. 8a: the intensity of the main band at 840 cm^{-1} decreased during storage as did the absorption intensity around 780 cm^{-1} (both indicative of $-Si(CH_3)_3$ groups). As the number of $-Si(CH_3)_3$ groups decreased, the number of $-Si(CH_3)_2-$ groups increased, as can be seen by the increase in absorption intensity at 810 cm^{-1} (methyl rock of $-Si(CH_3)_2-$). Finally, we point out the decrease in absorption of the NH bending vibration at 1180 cm^{-1} which was partially masked by the increase of the neighboring Si–O–Si stretching band.

Thus, FTIR data complement the XPS results. The main chemical changes observed (loss of silazane groups and formation of siloxane cross-links) are consistent with the fact that conventionally synthesized poly(organosilazanes) are highly reactive towards water or other protic solvents. Hydrolytic attack on the silazane moiety will liberate ammonia and produce the corresponding poly(organosiloxane) [24]. While our IR and XPS data indicate that an analogous process occurs in ppHMDSA, the oxidative changes on ageing must be more complex since the number of oxygen atoms incorporated was threefold the number of nitrogens lost. Also, hydrolytic conversion of silazane to the corresponding siloxane would not involve the loss of carbon which was clearly evident in XPS. Hence, oxidative ageing must also involve cleavage of Si–C and C–H bonds.

As for ppHMDSO, the formation of new siloxane links on ageing may proceed via silanol intermediates. In the ageing of ppHMDSA, however, IR data showed a much more pronounced loss of methyl groups from $-Si(CH_3)_3$ groups. Another reaction which operated in both plasma polymers is the abstraction of hydrogen from SiH moieties; this would also lead to the incorporation of siloxane cross-links in the ppHMDSA film. In contrast to the ppHMDSO findings, for ppHMDSA IR also provided evidence for hydrogen abstraction from methyl groups (generating methylene units) and the emergence of groups resulting from oxidation of hydrocarbon structures (carbonyl stretch). This was confirmed by XPS which indicated the formation of a range of carbon–oxygen functionalities (Fig. 7). This is probably a consequence of C–C bond formation during deposition and thus incorporation into this plasma polymer of a considerable amount of hydrocarbon segments, whereas for ppHMDSO the C is predominantly in the form of methyl groups rather than extended hydrocarbon chains. We have mentioned hydrogen abstraction from methyl groups in our discussion of the results obtained from the freshly deposited coating. A similar explanation is proposed for this continuing process: the structural data of the freshly deposited HMDSA plasma polymer suggested abstraction of hydrogen from Si–NH–Si groups in the glow discharge and the possible formation of branched structures such as Si(R1)–N(SiR2)–Si(R3) or

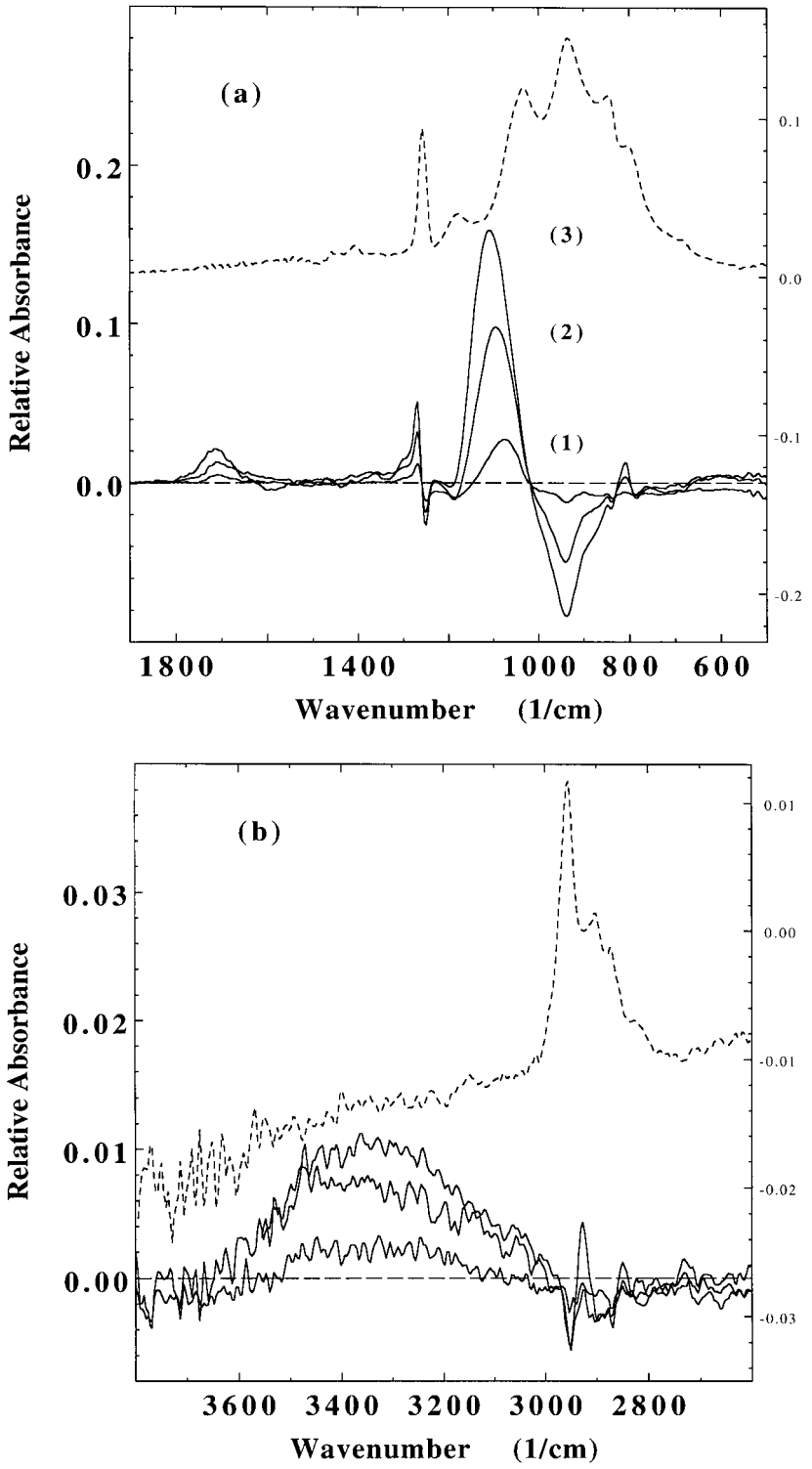

Fig. 8. IR difference spectra of the ppHMDSA film recorded at various times during storage: after 7 days (1), 66 days (2) and 575 days (3). Spectra recorded at intermediate times not shown. The spectrum of the freshly deposited coating is included for comparison (dashed curve). (a) low frequency region, (b) high frequency region.

Si(R1)–N(R2)–Si(R3). Si–N bond rupture as a result of oxidative/hydrolytic attack on these cross-links could generate $N^{\cdot}$ radicals which could form ammonia via hydrogen abstraction from surrounding methyl groups. Oxidation of the nitrogen-centred cross-links would eventually result in the incorporation of additional siloxanes and, in the case of Si(R1)–N(R2)–Si(R3), also amides by oxidation of the carbon atom of R2 adjacent to N.

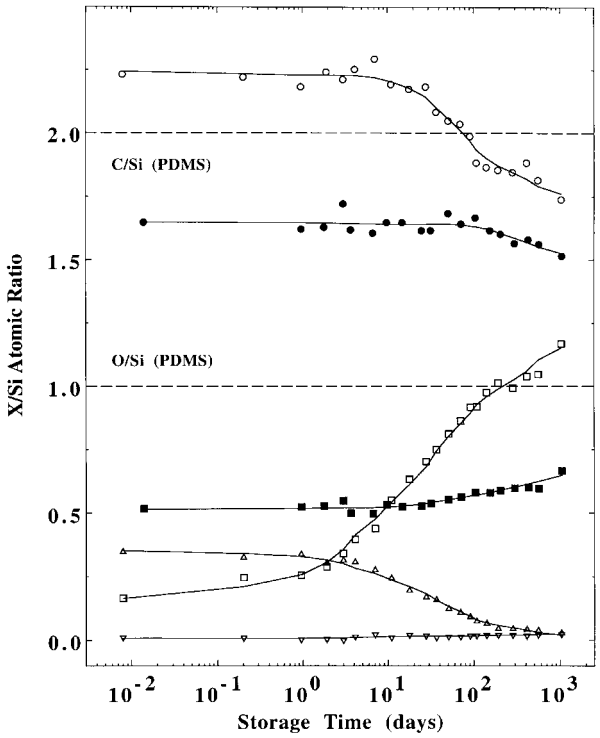

Fig. 9. XPS X/Si ratios as a function of storage time for ppHMDSA and ppHMDSO (measured at a photoelectron emission angle of 0°). Dashed lines mark the corresponding theoretical values for conventional PDMS. O/Si (ppHMDSO): ■; O/Si (ppHMDSA): □; C/Si (ppHMDSO): ●; C/Si (ppHMDSA): ○; N1/Si (ppHMDSA): △; N2/Si (ppHMDSA): ∇.

In summary, the ageing of ppHMDSO and ppHMDSA therefore compares as follows:

1. The ppHMDSO film underwent rather minor chemical changes on extended exposure to ambient air, with some incorporation of additional siloxane cross-links and a small extent of loss of methyl groups. Both the freshly deposited material and the aged coating showed an unusual extent of chemical homogeneity compared with the broad range of chemical structures typically found in most other plasma polymers.
2. The structure of the ppHMDSA coating was markedly affected by ageing, with about 50% of all silazane groups eliminated within one month and more than 90% after one year. Substantial amounts of oxygen were incorporated, with the O/Si ratio reaching that of PDMS (1.00) after only six months. As for ppHMDSO the

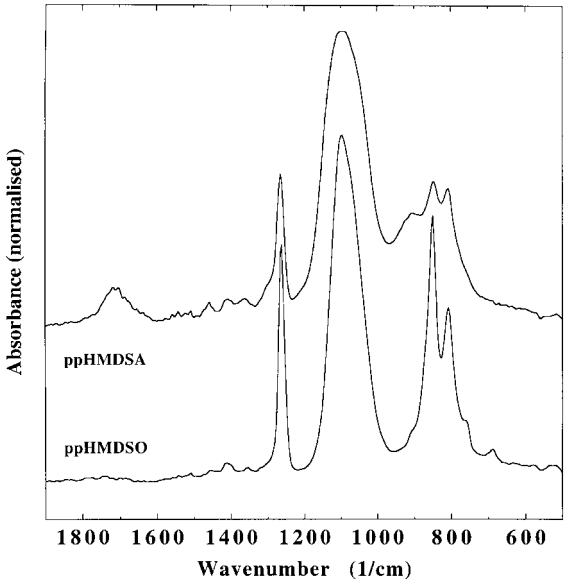

Fig. 10. Comparison of the IR spectra of the two aged plasma polymerised materials.

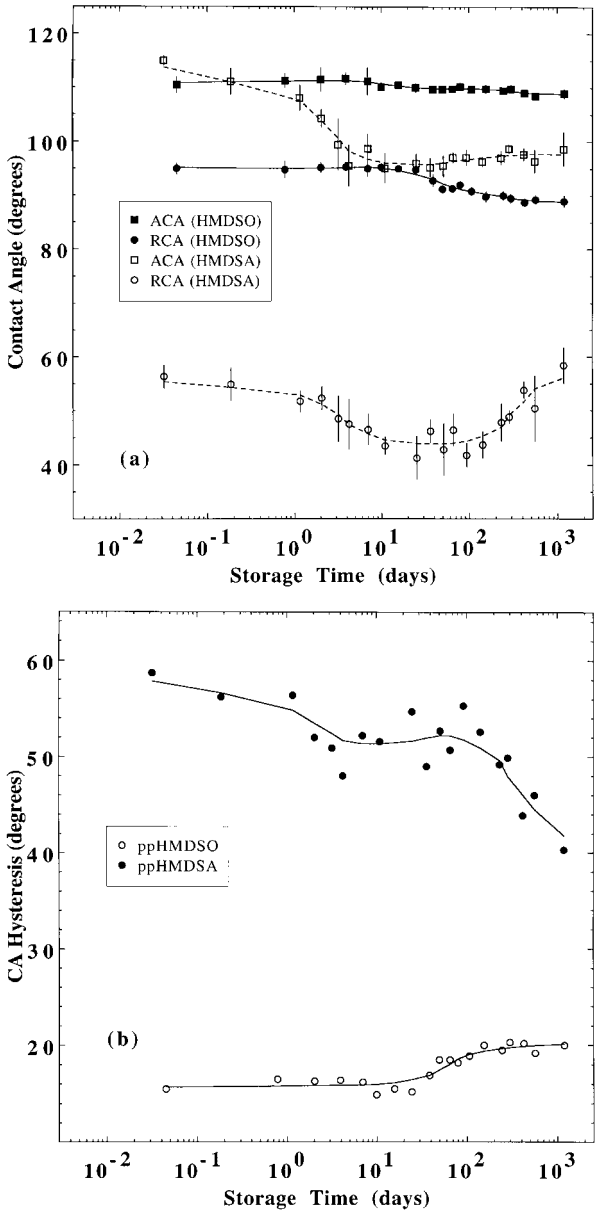

Fig. 11. Evolution of the water contact angles of the ppHMDSO- and ppHMDSA-surfaces as a function of storage time. (a) advancing (ACA) and receding (RCA) contact angle. (b) contact angle hysteresis measured on ppHMDSO (○) and ppHMDSA (●).

oxygen was mainly incorporated in the form of siloxane links.

3. In spite of the initial chemical differences, the two materials became more similar over time. This is illustrated in Fig. 9 which compiles the compositional data as recorded by XPS as a function of time for both coatings. The final structures of the aged materials were based on a cross-linked siloxane backbone. Carbon was mainly present in the form of methyl groups attached to silicon, although for ppHMDSA a range of other carbon-based groups were also detected. These groups (for example CH_2 and carbonyls) were a result of ageing following cleavage of C–H bonds, which appeared not to occur with ppHMDSO. Fig. 10 compares part of the IR spectra of the aged materials. The main vibrational bands in both cases are the Si–O–Si stretch and absorptions related to the $-Si(CH_3)_x-$ structure (methyl deformation at around 1260 cm $-$ 1 and methyl rock at approximately 850 cm^{-1} and 805 cm^{-1}). Most IR bands, in particular the band due to the Si–O–Si stretching vibration, and the Si 2p peak in XPS, were significantly broader for ppHMDSA, which is consistent with a greater diversity of chemical environments.

4.5. Effect on wettability of chemical changes due to ageing

The surface layers (outermost few nm) of polymeric materials may possess a composition that differs from that of the bulk material due to surface rearrangement motions caused by interfacial forces. As plasma polymers undergo oxidative changes during ageing, the interfacial energy situation changes. In addition, reaction-terminated diffusion of atmospheric O_2 causes an initially higher density of polar groups in the surface layers, and the resultant concentration gradient provides a further driving force for rearrangement motions that redistribute chemical groups over a depth scale that can be probed by angle-dependent XPS [25,40]. Redistribution motions in plasma polymer surface layers can also be manifested in contact angle data [25,40]. It is therefore of interest to study the interplay between oxidative ageing reactions and surface rearrangement motions.

Fig. 11 presents the changes in air/water contact angles (CAs) with time of the two plasma polymer surfaces. For comparison, Morra et al reported that CA values measured on PDMS were time dependent: the advancing CA decreased from 114° to 108° and the receding CA from 81° to 64° within 5 min of contact between water drop and solid surface; this bevaviour was ascribed to partial hydration of the polymer surface during measurement [41]. Other authors reported an advancing CA of 103° and a receding CA of 92° for spun bulk PDMS [39] and an advancing CA of 108° ± 3° for pure PDMS [42]. Our ppHMDSO is somewhat more hydrophobic, which may be the result of a lower oxygen content and the presentation of a high density of methyl groups at the interface.

The contact angle hysteresis (advancing minus receding) is unusually low for ppHMDSO, particularly since other plasma polymers have shown CA hysteresis considerably larger than for conventional polymers [25,40]. Contact angle hysteresis can be ascribed to a surface composition consisting of significant fractions of both hydrophobic and hydrophilic groups [43] and/or deviations from an ideal surface which should be smooth, homogeneous, rigid, and non-swelling [44]. In the present study, no evidence for hydration and swelling was observed. The measured hysteresis must therefore be interpreted as of thermodynamic rather than kinetic origin. Surface roughness of the plasma polymers films was assessed by atomic force microscopy (AFM). In the case of the ppHMDSO coating, the RMS roughness ranged between 1 nm and 2 nm. Roughness on this scale is not expected to contribute to hysteresis [45]. The hysteresis is therefore ascribed to chemical heterogeneity, which must be relatively small to account for the relatively low hysteresis. The high advancing CA suggests that mainly non-polar methyl groups were located at the surface during storage in air, possibly approaching a surface of close-packed methyl groups. The chemical heterogeneity of the surface is a result of the presence of a low density of polar structures (mainly siloxane groups), which have a greater effect on the receding CA.

The surface of the ppHMDSO film was relatively stable, with CAs slowly dropping after 1–2 weeks (Fig. 11), the receding CA more so than the advancing CA; hysteresis increased as a result from about 16° to 20°. For a hydrophobic surface the receding CA is particularly sensitive to small changes in the concentration of polar groups [44], and thus hysteresis increases with incorporation of additional polar groups. The CA changes with storage are consistent with the XPS and IR data (Figs. 2 and 4) showing an increase in the oxygen content and a reduction in the methyl group density. The chemical changes are relatively small and so are the CA changes; hence there is qualitative agreement. Quantitative correlations are not warranted given the different probe depths of XPS and CA measurements.

Freshly deposited ppHMDSA had a similar advancing CA (between 110° and 115°) but a much lower receding CA, of about 55°. The ppHMDSA surface was found by AFM to be significantly rougher than ppHMDSO, with values of the RMS roughness ranging between 5 nm and 6 nm. We have previously measured a slight increase of CA hysteresis on other plasma polymer surfaces due to roughness on this scale [45], and therefore assume that topography contributed to the CA hysteresis of the ppHMDSA coating, although the relatively large hysteresis must arise mainly from another origin. Since time-dependent contact angles did not indicate swelling to occur on a time scale of the measurements, we conclude that the hysteresis arose from the chemical structure at the surface of ppHMDSA being more heterogeneous than the surface of ppHMDSO (although the absolute fraction of polar structures was lower in the freshly deposited ppHMDSA coating than in ppHMDSO). We note that a higher degree of heterogeneity

Table 2
Atomic percentages measured at 75° divided by those acquired at 0°, and their time dependences

		%Si	%C	%O	%N
ppHMDSO	Fresh	0.995 ± 0.019	1.009 ± 0.009	0.975 ± 0.014	n/a
	Aged (3 years)	No change	No change	No change	n/a
ppHMDSA	Fresh	0.996 ± 0.014	1.013 ± 0.011	0.940 ± 0.018	1.02 ± 0.05
	Aged (3 years)	No change	No change	0.970 ± 0.018	1.20 ± 0.05

could be due to a greater difference in polarity of different species present and/or to a greater range of species.

Changes in contact angles over time were more extensive on the surface of the ppHMDSA film (Fig. 11). Both the advancing and the receding CA started to decrease immediately after deposition until they stabilised temporarily after about two weeks; the receding value started to increase again after several months reverting to the initial value after three years. Thus, in contrast to ppHMDSO, for ppHMDSA the CA hysteresis decreased during storage. Surface contamination by adventitious contaminants should not occur under our storage conditions and, moreover, could not account for the differences in the CA evolution of the two materials. Comparison with Fig. 5 shows that the CA decrease coincided with the rapid increase in XPS O/Si which was substantially larger than the simultaneous drop in N/Si, thus resulting in an overall higher fraction of polar surface entities. Interestingly, the hysteresis decreased at all times, particularly at long storage times (>3 months) when the receding CA increased again, even though the absolute concentration of polar (oxygen-containing) structures continued to increase.

Ideally, CA data should be correlated with angle-dependent XPS data and resultant compositional depth profiles. In the present cases however, we found the differences between XPS data collected at the two extreme emission angles (0° and 75° wrt the surface normal) to be relatively small, indicating that the calculation of quantitative depth profiles would be of limited usefulness and accuracy. Instead, we have used the atomic percentages collected at 75° divided by the corresponding values acquired at 0° as measures of compositional variations with depth. A value of 1 indicates uniform distribution of the respective species with depth below the surface, a value of greater (less) than 1 indicates a surface enriched (depleted) in the corresponding species. This method has previously been used to detect subtle rearrangements of polymeric segments at plasma polymer surfaces over time [25,40]. Table 2 summmarizes the results. For both coatings the slight carbon enrichment at the surface may be indicative of preferential orientation of methyl groups towards the air interface for reasons of interfacial energetics; we also observed a simultaneous slight depletion of oxygen although the latter was statistically not significant. In the case of ppHMDSO the ratios of the Si, C and O concentrations remained invariant during storage; these data indicate that oxidation was uniform throughout the top 10 nm of the material and that no slow surface rearrangement motions took place.

For ppHMDSA the distribution of Si and C was similarly uniform with depth and remained so over time. The depth distributions of N and O, on the other hand changed with time, with the surface becoming more enriched with these elements over time. The N enrichment at the surface increased gradually to ≈1.2 (data not shown) but due to the marked reduction in overall intensity of this element with time (Fig. 5) this did not have a significant effect on the depth distributions of the other elements.

The absence of even qualitative correlation between XPS data and CA hysteresis during ageing is puzzling, but the concept of surface restructuring provides a putative answer. On measurement of the advancing CA the probed surface is in equilibrium with air, essentially a non-polar medium. In measuring the receding CA, however, the contact line moves across a surface which had been in contact with water. While in the former case the surface is probably covered largely by methyl groups, in the latter case a higher concentration of polar structures, brought to the surface by rotational motions striving to minimize interfacial energy in contact with water, might be exposed at the surface. Thus, CA hysteresis might be due not only to chemical heterogeneity, but also to the (albeit limited) ability of the material to present different chemical groups at the surface depending on the contacting medium. This requires, of course, that such rotational motions be of a time scale within the time elapsed between advancing and receding CA measurements. Over time, however, the mobility of the plasma polymer may have been reduced due to the increasing formation of siloxane cross-links (as indicated by XPS and IR data). The reduced mobility of the surface layers hindered adaptive rotational motions of the surface on contact with water. An increasing proportion of hydrophobic methyl groups thus became immobilised at the surface, hence causing the receding CA to increase and the hysteresis to decrease, although more polar groups existed in the surface layers following oxidation

In summary, we conclude that the wettability data reflected the structural differences between the two materials. However, correlations between structures and surface properties were not predictable. A complex, time-dependent balance of various factors such as chemical structure, topography and mobility was responsible for the overall wettability of these surfaces.

5. Conclusions

HMDSO and HMDSA plasma polymer coatings were deposited under identical conditions. Whereas in the former case the siloxane unit was retained to a large extent, resulting in a relatively homogenous structure, Si–N bond cleavage and hydrogen abstraction from both silazane and methyl groups led to a more diverse structure of the ppHMDSA.

The long-term evolution during storage in air of the HMDSO-based material was found to be significantly different to that of other plasma polymers: the absence of any detectable incorporation of oxygen during the first few days after fabrication indicated that the freshly deposited coating did not contain an appreciable concentration of free radicals. The stability of the siloxane unit had a major influence during storage: XPS and FTIR detected only minor chemical changes which were ascribed to hydrolytic attack on Si–Si bonds and their subsequent replacement by additional siloxane cross-links. As a result, the material became more uniform and similar to its conventional analogue PDMS.

The structure of the freshly deposited ppHMDSA coating was found to be extremely unstable over time: a rapid increase in the concentration of oxygen and an almost complete loss of nitrogen was detected, starting immediately after fabrication. To a large extent, this dramatic difference between the two plasma polymers can be attributed to the presence of silazane bonds in the ppHMDSA; these are highly susceptible to hydrolytic decomposition which leads to their conversion to siloxane-based structures. In contrast to the ppHMDSO coating, oxidation of methyl and methylene groups also occurred which produced various carbon–oxygen and carbon–oxygen–nitrogen functional groups. Apart from the presence of these latter groups the IR data in particular showed the structure of the aged ppHMDSA to be rather similar to the ppHMDSO coating, both being based on a siloxane cross-linked network. In both cases, the structure of the aged material appeared to stabilise after one to two years.

The evolution of the wettability of ppHMDSO reflected the minor chemical changes detected during ageing with the surface becoming slightly more hydrophilic. The low degree of chemical heterogeneity resulted in a small CA hysteresis. In contrast, the ppHMDSA contact angle data confirmed the presence of a wider range of functional groups on the surface which had been detected spectroscopically: the CA hysteresis was found to be nearly fourfold that of the HMDSO analogue. As the materials became structurally more similar on ageing, the ratio of CA hystereses decreased to two. However, apart from these general trends, no simple correlations between structures and surface properties could be determined. A complex, time-dependent interplay of several factors obviously was responsible for the overall wettability of these surfaces. Based on the experimental evidence we identified chemical structure, topography and mobility as all playing a role in the evolution of the surface properties of the plasma polymerised coatings.

Acknowledgements

We thank Dr Heather StJohn and Dr Peter Kambouris for helpful discussions.

References

[1] Inagaki N, Kishi A. J Polym Sci, Polym Chem Ed 1983;21:2335.
[2] Inagaki N, Kondo S, Hirata M, Urushibata H. J Appl Polym Sci 1985;30:3385.
[3] Wróbel AM. J Macromol Sci-Chem 1985;A22:1089.
[4] Coopes IH, Griesser HJ. J Appl Polym Sci 1989;37:3413.
[5] Park SY, Kim N. J Appl Polym Sci: Appl Polym Symp 1990;46:91.
[6] Rochotzki R, Arzt M, Blaschta F, Kreyßig E, Poll HU. Thin Solid Films 1993;234:463.
[7] Matsuyama H, Kariya A, Teramoto M. J Membrane Science 1994;88:85.
[8] Matsuyama H, Shiraishi T, Teramoto M. J Appl Polym Sci 1994;54:1665.
[9] Ohuchi FS, Lin TJ, Antonelli JA, Yang DJ. Thin Solid Films 1994;245:10.
[10] Rau C, Kulisch W. Thin Solid Films 1994;249:28.
[11] Fonseca JLC, Barker CP, Badyal JPS. Macromolecules 1995;28:6112.
[12] Wang TF, Yasuda HK. J Appl Polym Sci 1995;55:903.
[13] Eufinger S, van Ooij WJ, Conners KD. Surf Interf Anal 1996;24:841.
[14] Zuri L, Silverstein MS, Narkis M. J Appl Polym Sci 1996;62:2147.
[15] Lamendola R, d'Agostino R, Fracassi F. Plasma and Polymers 1997;2:147.
[16] Bonnar MP, Wilson JIB, Burnside BM, Reuben RL, Gengenbach TR, Griesser HJ, Beamson G. Journal of Material Science, in press (1998).
[17] Wróbel AM, Wertheimer MR. Plasma-polymerized organosilicones and organometallics. In: d'Agostino R, editor. Plasma deposition, treatment, and etching of polymers. San Diego, CA: Academic Press, 1990.
[18] Gengenbach TR, Vasic ZR, Chatelier RC, Griesser HJ. J Polym Sci, Part A: Polym Chem 1994;32:1399.
[19] Gengenbach TR, Chatelier RC, Griesser HJ. Surf Interf Anal 1996;24:271.
[20] Gengenbach TR, Chatelier RC, Griesser HJ. Surf Interf Anal 1996;24:611.
[21] Gengenbach TR, Griesser HJ. J Polym Sci, Part A: Polym Chem, submitted (1998).
[22] Gengenbach TR, Griesser HJ. J Polym Sci, Part A: Polym Chem 1998;36:985.
[23] Gengenbach TR, Griesser HJ. Surf Interf Anal, in press (1998).
[24] Kricheldorf HR, editor. Silicon in polymer synthesis. New York: Springer, 1996.
[25] Gengenbach TR, Vasic ZR, Chatelier RC, Griesser HJ. Plasma and Polymers 1996;1:207.
[26] Harrison K, Hazell LB. Surf Interface Anal 1992;18:368.
[27] StJohn HAW, Griesser, HJ. Surf Interface Anal, submitted for publication.
[28] Beamson G, Briggs D. High resolution XPS of organic polymers. The Scienta ESCA300 database. 1st ed. Chichester, UK: John Wiley and Sons Ltd, 1992.
[29] Ban H, Sukegawa K. J Appl Polym Sci 1987;33:2787.
[30] Hirotsu T. J Appl Polym Sci 1957;1979:24.
[31] Tóth A, Bertóti I, Blazsó M, Bánhegyi G, Bognar A, Szaplonczay P. J Appl Polym Sci 1994;52:1293.

[32] Wagner DD, Powell CJ, Allison JW, Rumble JR. NIST X-ray photoelectron spectroscopy database. NIST standard reference database 20 version 2.0. US Department of Commerce, National Institute of Standards and Technology, Standard Reference Data Program, Gaithersburg, Maryland 20899, USA, 1997.
[33] Hughes AE, Sexton BA. J Electron Spectrosc Relat Phenom 1988;46:31.
[34] Bellamy LJ. The infrared spectra of complex molecules. Vol. 1, 3rd ed. New York: Halsted Press/John Wiley and Sons Ltd, 1975.
[35] Lin-Vien D, Colthup NB, Fateley WG, Grasselli JG. The handbook of infrared and Raman characteristic frequencies of organic molecules. 1st ed. San Diego, CA: Academic Press, 1991.
[36] Hummel DO, Scholl F. Atlas of polymer and plastics analysis. Vol. 2 b/I, 2nd ed. Munich: Carl Hanser Verlag, 1988.
[37] Zeigler JM, Gordon Fearon FW, editors. Advances in chemistry series, 224. Silicon-based polymer science. A comprehensive resource. Washington, DC: American Chemical Society, 1990.
[38] Pouchert CJ, editor. The Aldrich library of infrared spectra. 3rd ed. Milwaukee: Aldrich Chemical Company, 1981.
[39] Tsao M-W, Pfeifer K-H, Rabolt JF, Castner DG, Häussling L, Ringsdorf H. Macromolecules 1997;30:5913.
[40] Gengenbach TR, Vasic ZR, Li S, Chatelier RC, Griesser HJ. Plasma and Polymers 1996;2:91.
[41] Morra M, Occhiello E, Garbassi F, Marola R, Humphrey P. J Colloid Interface Sci 1990;137:11.
[42] Baier RE, Meyer AE. Biofouling 1992;6:165.
[43] Johnson RE, Dettre RH. Surf Coll Sci 1969;2:85.
[44] Garbassi F, Morra M, Occhiello E. Polymer surfaces. From physics to technology. 1st ed. Chichester, UK: John Wiley and Sons Ltd, 1994.
[45] Gengenbach TR. Unpublished results.